Transient-conductivity change induced by laser-pulsed excitation in semimetal films

J. C. G. de Sande

Departamento de Optica, Facultad de Ciencias Físicas, Universidad Complutense, 28040 Madrid, Spain

M. Sánchez Balmaseda

Departamento de Física Aplicada III (Electricidad y Electrónica), Faculdad de Ciencias Físicas, Universidad Complutense, 28040 Madrid, Spain

J. M. Guerra Pérez

Departamento de Optica, Facultad de Ciencias Físicas, Universidad Complutense, 28040 Madrid, Spain

An observation of photoconductivity in a homonuclear semimetal (bismuth) is reported. The effect is observed when bismuth films of different thicknesses are irradiated with 1.064-μm laser pulses. The sign and the temporal evolution of the resistivity change induced in the films are studied. An anomalous resistivity change due to laser heating is observed in the thickest film. A theoretical interpretation that explains and fits the experimental behavior well is given. The results support the predictions of a previously reported model that required the pumping of carriers into a metastable band by the laser light. The sum of the mobilities and of the diffusion coefficients for electrons and holes in this band are also estimated.

I. INTRODUCTION

Recently, an anomalous photoinduced effect in metal films has been reported. Current-biased samples were irradiated with short laser pulses and transient nanosecond voltages were measured. No complete and consistent explanation of the effect was given and, particularly, the possibility of a photoconductive effect was not considered.[1] On the other hand, time-resolving photoconductivity has been fairly well observed in different semiconductors.[2-5]

In previous publications we observed the anomalous response of bismuth films to irradiation with laser pulses. Thus, the Nernst-Ettingshausen effect induced by 1.064-μm laser pulses in bismuth films showed an unexpected behavior with the magnetic field and a classical dimensional effect with thickness.[6,7] A theoretical study was carried out to explain the temporal evolution of the thermomagnetic response of 5.5-μm bismuth films. A good fit to the experimental response was achieved only if an additional source term was included in the heat-diffusion equation: the one given by the electrons optically pumped to metastable states.[8] Further evidence of the existence of a metastable band was provided by the observation of the thermoelectric response of 5.5-μm bismuth films to two laser light wavelengths. The results were completely consistent with the metastable band hypothesis.[9] All of these works are in complete agreement with the spectroscopic observations of other authors that found in Bi a band peaked at 0.6 eV and an absorption edge for optical transitions located at about 0.3 eV, that is, below the 1.064-μm photons energy.[10-13]

The above-mentioned studies clearly show that the transport properties of the film change during irradiation. If optical pumping of carriers to a metastable con-

duction band is taking place, a transient photoconductivity effect must be detected in real time. As far as we know, photoconductivity has not been detected in intrinsic homonuclear conductors.

In this work, we report the measurement of transient photoconductivity induced by laser pulses in bismuth films with thicknesses 0.19, 0.95, and 4.3 μm. The laser irradiation produces a resistivity decrease for the three thicknesses. This result in the thickest film, where a temperature increase should produce a conductivity decrease, rules out a simple laser heating effect as the only process taking place in the irradiated films. In order to explain the sign as well as the temporal evolution of the resistivity changes observed in the films, two different effects have to be considered. The first is the mentioned increase of the carriers density in a metastable conduction band due to an optical pumping. The second is a surface effect as a consequence of the inhomogeneous heating of the sample. This last effect gives rise to a resistivity decrease even in the thickest film. With this interpretation, a good fit to the experimental registers is obtained. From the fit we estimate the sum of the electrons and holes mobilities in the metastable conduction band as well as the sum of their diffusion coefficients.

II. EXPERIMENT

Films were grown on glass substrates by vacuum evaporation (10^{-6} Torr) of 99.9999%-pure Bi. Before evaporation the substrates underwent a standard process of ultrasound cleaning. The film thickness was controlled by a quartz-crystal monitor during evaporation and later confirmed by a surface-profile analyzer. Samples of 0.19, 0.95, and 4.3 μm were evaporated at room temperature.

Bismuth films evaporated on glass substrates have a microcrystalline structure, the trigonal axis being perpendicular to the substrate and the binary axis being randomly oriented.[8]

The films were irradiated with a Q switched and polarized Nd-YAG laser. A typical impinging laser pulse had a temporal width between 15 and 20 ns. The energy is assumed to be evenly distributed over a transversal section of $\simeq 14.0 \pm 1.5$ mm^2, where the sample was placed. The energy was attenuated by the joint effect of three or more neutral filters down to energy densities of $\simeq 75$, 55, and 20 J/m^2 for 4.3-, 0.95-, and 0.19-μm films, respectively. The precision of the energy density values is affected by the uncertainty in the energy distribution on the laser spot area and of the transmission coefficient of the neutral filters stack. This uncertainty could attain a maximum value of $\simeq 30\%$.

A beam splitter was used to divide the laser beam. The first of these beams was detected by a < 1 ns-rise time photodiode to be used as a monitorizing signal. This first beam was also used to synchronize a transient programmable digitizer, its 3-dB bandwidth being 600 MHz. The second beam fell perpendicularly on the film surface. The electrical signals generated in the film were registered in the mentioned digitizer.

Transient resistivity changes were measured by a four-points method with time-resolving capability. A small change in the sample resistance ΔR will produce a signal

$$\Delta V_b = V_b \frac{\Delta R}{R} \frac{R_e}{R_e + R} , \tag{1}$$

where V_b is the voltage across the sample produced by the bias current intensity and R_e is the equivalent resistance of the bias generator internal resistance connected in parallel with the oscilloscope input impedance.

The films were biased by a long current pulse (≈ 100 μs width) synchronized with the laser pulse. The current intensity was less than 0.5 A. This current would produce a maximum temperature increase of 5 K, which corresponds to the case of the thinnest film. But, during the typical duration of the measurement (500 ns), this temperature increase is always below 0.01 K. Then, the sample temperature can be taken essentially independent of the bias current in the measurement time scale. The room temperature during the measurements was 295 K. In order to measure the resistivity changes induced by the laser light, the film bias signal was filtered through a capacitor in series. This allowed us to eliminate the slowly varying signals and to measure the fast signals on a more sensitive scale. The signals generated in the films passed through the capacitor and were finally registered in the transient digitizer. All the transmission lines were coaxial and impedance matched at 50 Ω. A detailed study of this setup can be found in Ref. 14.

III. RESULTS

As is well known, the resistivity of bulk bismuth increases steadily with the temperature.[15,16] Nevertheless, the resistivity of bismuth films decreases or increases as

temperature increases depending on the film thickness as well as on the temperature range. Usually, the resistivity exhibits a broad minimum at a certain temperature. This temperature depends on the film thickness. Since from the available literature data it is not clear what would be the foreseeable behavior for our particular set of bismuth films,[15-25] we measured the temperature dependence of resistivity for different thicknesses. Figure 1 shows the plot of resistance versus temperature for films with thicknesses of 0.22, 1.2, and 4.3 μm. The evaporation conditions for these films were those described in Sec. II. As it can be observed, between 290 K and 330 K, the resistance of the 0.22-μm (4.3-μm) film decreases (increases) as temperature increases. The resistance of the 1.2-μm film shows a minimum in this temperature range. This behavior has to be known in order to interpret the results obtained when the films are irradiated and described hereafter.

The real temporal width of the photoinduced signal is somewhat longer than the one registered due to the filtering through the series capacitances. The distortion introduced by the filtering system can be eliminated integrating the registered signal $\Delta V(t)$ in the following way:

$$\Delta V_b(t) = \Delta V(t) + \int_0^t \frac{\Delta V(t')}{R_0 C} dt' , \tag{2}$$

where $\Delta V_b(t)$ would be the real induced signal, R_0 is the oscilloscope impedance, and C the total capacitance of the filter plus the preamplifier.[26]

The film response to the laser pulse $\Delta V_b(t)$ is shown in Figs. 2(a), 3(a), and 4(a) for each sample. Curves have the maximum value normalized to unit. The plotted signals correspond to the mean value of five measurements. In order to cancel the small transverse thermoelectrical signals of the films, each measurement is the difference between two individual registers, one taken with a given direction of the bias current and the other taken with the bias current in the opposite direction.[9] In spite of the electrical isolation given by the Faraday cage, some repetitive stray field and line reflections modulate the registered signal. This is due to the mismatch between the sample and the coaxial line impedances. The peak of the relative resistivity change for each film is obtained substituting the voltage change measured in the maximum of ΔV_b in Eq. (1). Table I collects these peak values $\Delta \rho_m / \rho_0$, where ρ_0 is the resistivity of the film before
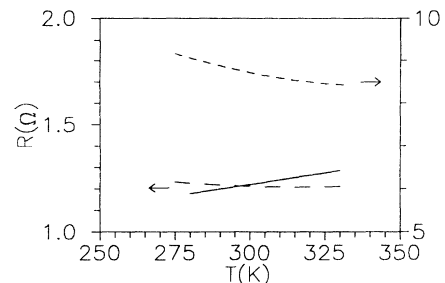
FIG. 1. Resistance versus temperature for (——) 4.3-μm, (– – –) 1.2-μm, and (- - - -) 0.22-μm Bi films.

TABLE I. Parameter values used in the calculations and in the fits for each film.

d (μm)	$\Delta\rho_m/\rho_0$ (Experimental)	$\Delta\rho_m/\rho_0$ (Calculated)	b_1	b_2	ρ_0 (Ω m)	$\Delta\rho_{pm}/\rho_0$	$\tau_e/(m_e^*/m_0)+$ $\tau_h/(m_h^*/m_0)$(s)
4.3	-1.5×10^{-3}	-1.8×10^{-3}	0.68	0.44	1.20×10^{-6}	-7.8×10^{-4}	1.2×10^{-15}
0.95	-6.5×10^{-3}	-5.8×10^{-3}	0.87	0.30	1.35×10^{-6}	-1.7×10^{-3}	0.75×10^{-15}
0.19	-2.9×10^{-2}	-1.5×10^{-2}	0.66	0.38	2.0×10^{-6}	-5.6×10^{-3}	0.83×10^{-15}

irradiation. As can be observed, all the films' responses correspond to a negative resistivity change. This result in the 4.3-μm film clearly shows that the laser light is producing an effect opposite in sign to the one expected by a simple heating of the film.

IV. THEORETICAL INTERPRETATION

When the Thèvenin equivalent of the film is calculated, an internal resistance is found given by

$$R = \left(\int_0^d \frac{\sigma(x)}{c} dx\right)^{-1}, \qquad (3)$$

where d is the film thickness, $\sigma(x)$ is the electrical conductivity of the film, x is the coordinate along the beam direction, and c is an adimensional geometrical factor.[9]

As it has been mentioned, we have previously observed that when a bismuth film is irradiated with 1.064-μm photons, carriers are pumped to a metastable conduction band.[8,9] Since the laser radiation produces a temperature increase and a nonthermal enhancement in the free carriers density, the electrical conductivity at a given instant t can be written as

$$\sigma(x,t) = \sigma_0 + \Delta\sigma(x,t), \qquad (4)$$

where σ_0 is the film electrical conductivity at room temperature and $\Delta\sigma(x,t)$ is the electrical conductivity change due to the laser irradiation. As this change is very small we can approximate the variation of the resistivity as follows:

$$\frac{\Delta\rho(t)}{\rho_0^2} \simeq 1/\rho_0 - 1/\rho(t) = -\int_0^d \frac{\Delta\sigma(x,t)}{d} dx. \qquad (5)$$

The conductivity change $\Delta\sigma(x,t)$ is assumed to be due to two different effects: the heating of the film and the presence of carriers in the conduction metastable band.

A. Optically pumped carriers effect

The temporal evolution of the pumped carriers density is given by

$$n(x,t) = n_e(x,t)$$
$$= n_h(x,t) = \frac{\phi_0 \exp^{-\delta x/d}}{h\nu_L}$$
$$\times \int_0^t f(t') \exp^{-(t-t')S_m} dt',$$
$$\phi_0 = \frac{A w_r \delta}{d(1 - \exp^{-\delta}) \int_0^\infty f(t)dt}, \qquad (6)$$

FIG. 2. Temporal evolution of the resistivity change for the 4.3-μm Bi film. (a) (———): Experimental response; (- - - -): theoretical response given by Eq. (18); (b) (———): $\Delta\rho_p$; (- - - -): $\Delta\rho_t$; (— — —): $\Delta\rho_a$. The curves are normalized to unit.
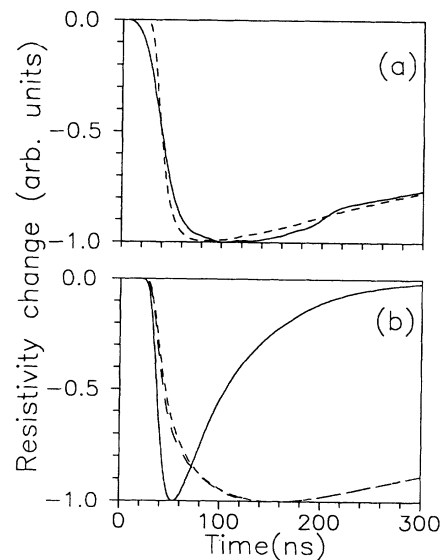
FIG. 3. Temporal evolution of the resistivity change for the 0.95-μm Bi film. (a) (———): Experimental response; (- - - -): theoretical response given by Eq. (18); (b) (———): $\Delta\rho_p$; (- - - -): $\Delta\rho_t$; (— — —): $\Delta\rho_a$. The curves are normalized to unit.
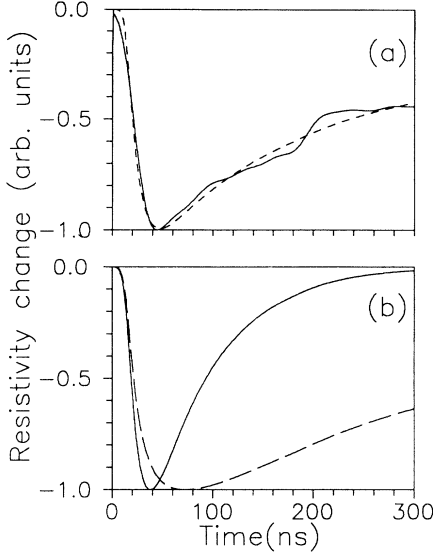
FIG. 4. Temporal evolution of the resistivity change for the 0.19-μm Bi film. (a) (——): Experimental response; (- - - -): theoretical response given by Eq. (18); (b) (——): $\Delta\rho_p$; (- - - -): $\Delta\rho_t$; (– – –): $\Delta\rho_a$. The curves are normalized to unit.

where $n_e(x,t)$ and $n_h(x,t)$ are the density of pumped electrons and holes respectively, $\delta = d/x_L$, where x_L is the attenuation distance of the laser radiation in the material, $f(t)$ the temporal profile of the laser pulse, $h\nu_L$ the photon energy, A the absorption coefficient, S_m the recombination rate of the pumped carriers, and w_r is the energy density per unit of area and per pulse.[8] To evaluate $n(x,t)$, the following parameters were used: $x_L = 20$ nm, $A = 0.33$, and $S_m^{-1} = 57$ ns.[9,27] This calculation yields values for n ($x \gtrsim 10x_L$, 300 ns $> t > t_0$) always bigger than 10^{22} m^{-3}, t_0 being the laser-pulse half width. This means that local thermodynamic equilibrium can be assumed.[28] Thus, the conductivity change due to the optically pumped carriers can be written in this way:

$$\Delta\sigma_p(x,t) = \sigma_e(x,t) + \sigma_h(x,t)$$

$$= \frac{e^2}{m_0} \left(\frac{\tau_e}{m_e^*/m_0} + \frac{\tau_h}{m_h^*/m_0} \right) n(x,t) , \qquad (7)$$

where the subscripts e and h refer to electrons and holes, respectively, e is the absolute electron charge, m_0 is the rest electron mass, and τ and m^* are the relaxation time and the effective mass, respectively. Using Eq. (5), we have the corresponding resistivity change:

$$\frac{\Delta\rho_p(t)}{\rho_0^2} = - \frac{e^2}{m_0} \left(\frac{\tau_e}{m_e^*/m_0} + \frac{\tau_h}{m_h^*/m_0} \right) \int_0^d \frac{n(x,t)}{d} dx .$$

$$(8)$$

Figures 2(b), 3(b), and 4(b) show that $\Delta\rho_p(t)$ is negative in the three films, as the measured resistivity changes, but its temporal evolution does not follow the temporal evolution of the induced signals.

B. Thermal effect

As is well known, a change in the sample conductivity due to a temperature change is given by

$$\Delta\sigma_t(x,t) = \alpha\Delta T(x,t) , \qquad (9)$$

where $\alpha = d\sigma/dT$ and $\Delta T(x,t)$ is the temperature change of the film at a given instant t and at any position x. The temperature distribution is the solution of the known heat-diffusion equation:

$$\rho' c_p \frac{\partial T}{\partial t} = \phi' + K_t \frac{\partial^2 T}{\partial x^2} , \qquad (10)$$

where ρ' is the mass density, c_p the specific heat, K_t the thermal conductivity, and ϕ' the source term that can be written as

$$\phi' = \phi_0 \exp(-\delta x/d) f'(t) , \qquad (11)$$

with $f'(t)$ expressed by

$$f'(t) = \left(1 - \frac{E_m}{h\nu_L} \right) f(t)$$

$$+ \frac{E_m}{h\nu_L} S_m \int_0^t f(t') \exp[-S_m(t - t')]dt' , \qquad (12)$$

where E_m is the average recombination energy of the pumped carriers. The source term ϕ' takes into account the effect of the heat liberated during the time that the recombination of pumped carriers takes place.[8,9] We have solved this equation by means of a standard numerical method where the heat diffusion through the substrate has been considered.[29] In this calculation, we have used the experimental register of the laser pulse for $f(t)$ and taken $E_m \simeq 0.64$ eV.[8,9] Under our experimental conditions, the rise of temperature is always below 30 K, even near the film surface. Figure 1 shows that α is practically constant in the measured temperature range, so we can write

$$\frac{\Delta\rho_t(t)}{\rho_0^2} = -\alpha \int_0^d \frac{\Delta T(x,t)}{d} dx . \qquad (13)$$

The described calculation gives the temporal evolution of the resistivity change $\Delta\rho_t$ shown in Figs. 2(b), 3(b), and 4(b). It must be noticed that α is negative for the thickest film.

The solution of the heat-diffusion equation without considering the effect of the metastable band carriers recombination, yields a temporal evolution of the thermal resistivity change quite different from the measured one for each film.

When comparing Figs. 2(a) and 2(b), it is easily observed that the measured resistivity change cannot be fitted by the addition of the two contributions given by Eqs. (8) and (13). Obviously, the thermal contribution given by Eq. (13) cannot account for the experimental behavior of the resistivity change either. The temporal profiles shown in Fig 2(b) suggest that, in order to obtain the experimental evolution of $\Delta\rho$ in the thickest film, an

additional and unexpected negative contribution besides $\Delta \rho_p$ is taking place in the phenomenon. We must note that the laser pulse does not heat the sample in a homogeneous way and that in the neighborhood of the film surface a conductivity size effect is foreseeable. Thus, it can be expected that this temperature increase gives a different contribution than that of Eq. (13), which ignores a possible size effect.

To prove the reability of this interpretation we propose a simple model. The film is roughly divided into two parts: a superficial and hot slice of thickness $d_s(t)$ and the rest of the film at room temperature. We take $d_s(t)$ as the depth where the temperature increase is the ratio $\Delta T_m(t)/2$ and where $\Delta T_m(t)$ is the maximum temperature increase (see Fig. 5). The main thermal-induced resistivity change would take place in this thin slice. In this model, we assume that the coefficient α is one of a film of thickness $d_s(t)$. Thus the sample resistance R would be the equivalent of two resistances associated in parallel

$$\frac{1}{R} = \frac{d_s(t)[\sigma_0 + \Delta\sigma_s(t)]}{c} + \frac{[d - d_s(t)]\sigma_0}{c} , \quad (14)$$

where $\Delta\sigma_s(t)$ is the conductivity change in the hot slice. Here we can take $\Delta\sigma_s(t) \simeq \alpha(d_s)\Delta T_s(t)$, where $\Delta T_s(t)$ is the mean temperature increase in the thickness d_s. A simple calculation leads to an anomalous thermal-induced change in the resistivity given by

$$\frac{\Delta\rho_a(t)}{\rho_0^2} = -\alpha(d_s(t))\Delta T_s(t)d_s(t)/d . \quad (15)$$

From the current literature, it is possible to find the behavior of α with the film thickness. The experimental data of other authors[15-25] and those obtained from our resistance versus temperature measurements are plotted in Fig. 6. An empirical expression for α that fits the behavior of the collected data with thickness is

$$\alpha(d) = \alpha_0 \left(1 + \frac{a_1}{a_2 d + 1} \right) , \quad (16)$$

where α_0 is the corresponding coefficient for the bulk material at room temperature and a_1 and a_2 are fitting parameters. Some authors give theoretical expressions for $\alpha(d)$ that fit their own experimental data measured in a very narrow range of thicknesses well.[20,25] In both cases
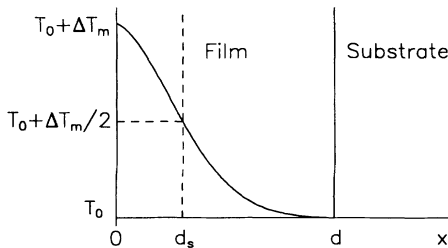
their expressions do not account for the value of α corresponding to thick films and bulk material. Equation (16) agrees with the behavior of $\alpha(d)$ for thick films predicted by the Fuchs-Sondheimer theory well.[30] The curve $\alpha(d)$ drawn in Fig. 6 corresponds to a fit with $a_1 \simeq -1.16$, $a_2 \simeq 6.83 \times 10^4$ m^{-1} and with a value $\alpha_0 \simeq -3.7 \times 10^3$ Ω^{-1}K^{-1} m^{-1}, which is the average of five reported values.[15,16,25,31,32] The function $\alpha(d)$ changes in sign at a thickness $\simeq 2.3$ μm.

Introducing $\alpha(d)$ in Eq. (15) and calculating $\Delta T_s(t)$ by means of Eq. (10), we obtain $\Delta\rho_a(t)$. Figure 2(b) shows this result for the 4.3 μm film. This contribution to the resistivity change is negative, but does not follow the temporal evolution of the measured resistivity change.

Nevertheless, a good fit to the experimental results is achieved if the contributions given by Eqs. (8) and (15) are both considered:

$$\Delta\rho(t) = \Delta\rho_a(t) + \Delta\rho_p(t) . \quad (17)$$

As we have normalized the resistivity changes to unity, it is convenient to rewrite Eq. (17) in the form:

$$\frac{\Delta\rho(t)}{|\Delta\rho_m|} = b_1\frac{\Delta\rho_a(t)}{|\Delta\rho_{am}|} + b_2\frac{\Delta\rho_p(t)}{|\Delta\rho_{pm}|} , \quad (18)$$

where

$$b_1 = \left|\frac{\Delta\rho_{am}}{\Delta\rho_m}\right|, \qquad b_2 = \left|\frac{\Delta\rho_{pm}}{\Delta\rho_m}\right| , \quad (19)$$

and $\Delta\rho_m$, $\Delta\rho_{am}$, and $\Delta\rho_{pm}$ are the peak values of $\Delta\rho(t)$, $\Delta\rho_a(t)$, and $\Delta\rho_p(t)$, respectively.

The final fit to the experimental resistivity change attained with Eq. (18) in the 4.3-μm film can be seen in Fig. 2(a). Figures 3(a) and 4(a) show this same fit for the rest of the films. The particular contributions $\Delta\rho_t(t)$, $\Delta\rho_a(t)$, and $\Delta\rho_p(t)$ are given in Figs. 3(b) and 4(b). The values b_1 and b_2 obtained from the fits are listed in Table I.

Observing Figs. 3 and 4, it is clear that the temporal evolution of the experimental resistivity change in the corresponding films cannot be explained only by the effect of the sample heating. In order to explain these profiles, it is necessary to consider the conductivity enhancement produced by the pumped carriers. On the

FIG. 5. Temperature distribution along the film thickness at a given instant. T_0 is the film temperature before irradiation.
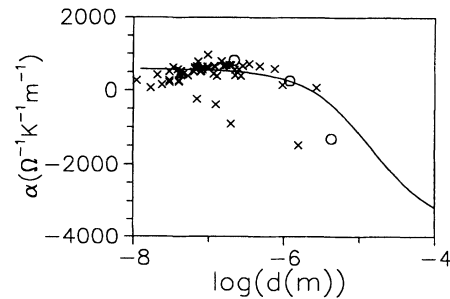
FIG. 6. The coefficient α versus $\log_{10}(d)$. (×): collected data from the literature; (o): measured data; (———): $\alpha(d) = \alpha_0[1 + a_1/(a_2d + 1)]$, being $\alpha_0 \simeq -3.7 \times 10^3$ Ω^{-1}K^{-1} m^{-1}, $a_1 \simeq -1.16$, and $a_2 \simeq 6.83 \times 10^4$ m^{-1}.

other hand, the thermal temporal evolutions predicted by Eq. (13) and those predicted by Eq. (15) are practically the same for the film of 0.19 μm and slightly different for the 0.95-μm film. This is due to the fact that the thinner the film is, the more uniform the spatial temperature distribution is and the shorter the time in which d_s becomes equal to the film thickness is.

Making use of Eq. (15) and taking ρ_0 from the literature,[15,19,24,33,34] $\Delta\rho_{am}/\rho_0$ can be evaluated. With the value $\Delta\rho_{am}/\rho_0$ and those of b_1 and b_2 for each particular film, and comparing Eqs. (17) and (18), the values $\Delta\rho_m/\rho_0$ and $\Delta\rho_{pm}/\rho_0$ can be calculated. Table I shows that the peaks of the resistivity changes $\Delta\rho_m/\rho_0$ thus calculated are similar to the measured ones. The discrepancies can be explained by the uncertainties in the measurement of the energy densities except perhaps in the case of the 0.19-μm film. For this film the value of α given by Eq. (16) is $\alpha \simeq 530 \ \Omega^{-1}\,\mathrm{K}^{-1}\,\mathrm{m}^{-1}$, much lower than the one measured by us $\alpha \simeq 820 \ \Omega^{-1}\,\mathrm{K}^{-1}\,\mathrm{m}^{-1}$ for a similar film. Using the measured value of α we obtain $\Delta\rho_m/\rho_0 \simeq -2.3 \times 10^{-2}$, which is closer to the experimental value.

Substituting the values of $\Delta\rho_{pm}/\rho_0$ in Eq. (8), we can obtain $\tau_e/(m_e^*/m_0) + \tau_h/(m_h^*/m_0)$ (see Table I). To do this calculation, the use of ρ_0 and w_r is not necessary. Averaging the three values obtained we can estimate the sum of the pumped carriers mobilities

$$\mu_e + \mu_h = \frac{e}{m_0}\left(\frac{\tau_e}{(m_e^*/m_0)} + \frac{\tau_h}{(m_h^*/m_0)}\right)$$
$$\sim 1.6 \times 10^{-4}\mathrm{m}^2\,\mathrm{V}^{-1}\,\mathrm{s}^{-1}\,. \qquad (20)$$

Bearing in mind Einstein's relation, the diffusion coefficients of the pumped carriers are obtained in the form:

$$D_e + D_h = \frac{K_B T}{e}(\mu_e + \mu_h) \sim 4 \times 10^{-6}\,\mathrm{m}^2/\mathrm{s}\,. \qquad (21)$$

The estimation given in Eq. (20) means that both mobilities are much lower than those of the intrinsic bismuth carriers.[21,22,31,35,36] The same argument is applied to the diffusion coefficients. This result supports the assumption, made in a previous work, that during the recombination time the slowest kind of pumped carriers, at least, does not spread excessively.[9]

Recently, several works have been published that deal with the band structure of bismuth. The metastable band which we have referred to in this work and in previous ones, could be identified in principle with one of the three following bands: T_6^+, T_6^-, or T_{45}^+.[37] All these bands, as well as the valence band T_{45}^-, have their origin in the Hartree p level of the atomic structure. Thus any of the direct transitions between two of these bands violates the selection rule $\Delta l = \pm 1$ and some degree of metastabil-

ity can be expected. Theoretical calculations establish the edge of the T_6^+, T_6^-, and T_{45}^+ bands in 0.77, 1.11, and 1.50 eV, respectively,[37] or in 0.49, 1.00, and 1.33 eV, respectively,[38] all the values above the Fermi level. These theoretical calculations are usually performed to fit the overlap between the L_s and T_{45}^- bands (where electrons and holes lie), the predictions for the excited states being less precise.

There are some experimental data about a band absorption edge in bismuth although they present a large dispersion. Thus, Omaggio et al.[39] find the T_6^+ band edge at 0.407 eV by infrared magnetotransmission measurements. High-resolution electron-energy-loss spectroscopy studies give a value of 0.20 eV for the same band edge.[40] An absorption edge in the range 0.17–0.30 eV has been found from spectroscopic measurements.[10-13] These values could correspond to the absorption edge of the T_6^+ band.

In our experiment, we irradiate the samples with 1.17-eV photons and probably excite electrons from the Fermi level of the T_{45}^- band to high levels of the T_6^+ band or, perhaps, to levels of the T_6^- band. From our experimental results, the average recombination energy of excited carriers to the T_{45}^- band is about 0.6 eV.[8,9] This implies that a cascade of very fast intraband nonradiative transitions takes place before the recombination. Then it seems reasonable to assume that the main part of the recombinations takes place from the levels of the lower band T_6^+.

V. CONCLUSIONS

A transient conductivity change has been measured in bismuth films of different thicknesses by excitation with 1.064-μm laser pulses. The experimental results reveal that photoconductivity is being induced and that an anomalous resistivity change produced by the laser light heating is taking place in the films. The measured resistivity changes have been well explained by a theoretical interpretation that takes into account the enhancement of carriers in a superior metastable band and the influence of a surface effect due to the inhomogeneous heating of the films. From the fitting between the theoretical and the experimental results, a rough estimation is given for the sum of the mobilities and the sum of the diffusion coefficients of electrons and holes in the metastable conduction band.

ACKNOWLEDGMENTS

[1] M. Johnson, M. R. Beasley, T. H. Geballe, S. R. Greenfield, J. J. Stankus, and M. D. Fayer, Appl. Phys. Lett. **58**, 568 (1991).

[2] J. W. Orton and P. Blood, *The Electrical Characterization of Semiconductors: Measurements of Minority Carriers Properties* (Academic Press, London, 1990).

[3] G. J. Galvin, M. O. Thompson, J. W. Mayer, R. B. Hammond, N. Paulter, and P. S. Peercy, Phys. Rev. Lett. **48**, 33 (1982).

[4] G. Yu, A. J. Heeger, G. Stucky, N. Heron, and E. M. Car-

ron, Solid State Commun. **72**, 345 (1989).

[5] M. Kunst, H. C. Neizert, and H. Ruebel, Phys. Rev. B **44**, 1081 (1991).

[6] J. M. Guerra and M. Sánchez Balmaseda, Phys. Rev. B **33**, 3745 (1986).

[7] M. Sánchez Balmaseda and J. M. Guerra, Phys. Rev. B **40**, 8252 (1989).

[8] M. Sánchez Balmaseda and J. M. Guerra, Phys. Rev. B **41**, 10 372 (1990).

[9] J. C. G. de Sande, M. Sánchez Balmaseda, and J. M. Guerra Pérez, Phys. Rev. B **47**, 9844 (1993).

[10] J. N. Hodgson, Proc. Phys. Soc. London Sect. B **67**, 269 (1954).

[11] A. P. Lenham, D. M. Treherne, and R. J. Metcalfe, J. Opt. Soc. Am. **55**, 1072 (1965).

[12] S. Mahmoud, Fizika (Zabreg) **18**, 243 (1986).

[13] H. T. El-Shair, M. I. El-Agrab, M. M. El-Nahass, A. M. Ibrahim, M. H. Ibrahim, and El-Shazly, Opt. Pura Aplicada **24**, 23 (1991).

[14] J. C. G. de Sande, M. Sánchez Balmaseda, and J. M. Guerra Pérez, Rev. Sci. Instrum. (to be published).

[15] R. A. Hoffman and D. R. Frankl, Phys. Rev. B **3**, 1825 (1971).

[16] C. Pariset, Thin Solid Films **91**, 301 (1982).

[17] Y. F. Komnik, E. I. Bukhshtab, Y. V. Nikitin, and V. V. Andrievskii, Zh. Eksp. Teor. Fiz. **60**, 669 (1971) [Sov. Phys. JETP **33**, 364 (1971)].

[18] N. García, Y. H. Kao, and M. Strongin, Phys. Rev. B **5**, 2029 (1972).

[19] Y. F. Komnik and V. V. Andrievsky, Thin Solid Films **42**, 1 (1977).

[20] W. Schnelle and U. Dillner, Phys. Status Solidi A **44**, 197 (1977).

[21] S. Kochowski and A. Opilski, Thin Solid Films **48**, 345 (1978).

[22] A. H. de Kuijper and J. Bisschop, Thin Solid Films **110**, 99 (1983).

[23] W. Schnelle and U. Dillner, Phys. Status Solidi A **115**, 505 (1989).

[24] A. Kumar and O. P. Katyal, J. Mat. Sci. Mat. Electron. **1**, 51 (1990).

[25] A. Kumar and O. P. Katyal, Appl. Phys. A **52**, 265 (1991).

[26] P. Horowitz and W. Hill, *The Art of Electronics*, 2nd ed. (Cambridge University Press, Cambridge, England, 1989).

[27] *AIP Handbook*, 3rd ed., edited by Dwight E. Gray (AIP, New York, 1972).

[28] *Electrical Breakdown and Discharges in Gases, Macroscopic Processes and Discharges*, Vol. 89b of *NATO Advanced Study Institute Series B: Physics*, edited by E. E. Kunhardt and L. H. Luessen (Plenum Press, New York, 1983).

[29] W. Kreith, *Basic Heat Transfer* (Harper & Row, New York, 1980).

[30] E. H. Sondheimer, Adv. Phys. **1**, 1 (1952).

[31] C. F. Gallo, B. S. Chandrasekar, and P. H. Sutter, J. Appl. Phys. **34**, 144 (1963).

[32] J. P. Issi, J. P. Michenaud, and J. Heremans, Phys. Rev. B **14**, 5156 (1976).

[33] S. Baba, H. Sugawara, and A. Kinbara, Thin Solid Films **31**, 329 (1976).

[34] A. Kawazu, Y. Saito, H. Asahi, and G. Tominaga, Thin Solid Films **37**, 261 (1976).

[35] L. K. J. Vandamme and J. Kedzia, Thin Solid Films **65**, 283 (1980).

[36] U. Dillner and W. Schnelle, Phys. Status Solidi A **116**, 715 (1989).

[37] J. H. Xu, E. G. Wang, C. S. Ting, and W. P. Su, Phys. Rev. B **48**, 17 271 (1993).

[38] X. Gonze, J. P. Michenaud, and J. P. Vigneron, Phys. Rev. B **41**, 11 827 (1990).

[39] J. P. Omaggio, J. R. Meyer, C. A. Hoffman, A. DiVenere, X. J. Yi, C. L. Hou, H. C. Wang, J. B. Ketterson, G. K. Wong, and J. P. Heremans, Phys. Rev. B **48**, 11 439 (1993).

[40] V. De Renzi, M. Grazia Betti, and C. Mariani, Phys. Rev. B **48**, 4767 (1993).